JOURNAL OF Materials CHEMISTRY

Synthesis, properties and structural characterization of an intermolecular photosensitive complex: $(HGly\text{-}Gly)_3PMo_{12}O_{40}\cdot 4H_2O$

Zhengbo Han,[a] Enbo Wang,*[a] Guoyou Luan,[a] Yangguang Li,[a] Hong Zhang,[a] Yingbo Duan,[a] Changwen Hu[a] and Ninghai Hu[c]

[a]*Department of Chemistry, Northeast Normal University, Changchun 130024, P. R. China. E-mail: wangenbo@public.cc.jl.cn*
[b]*Northeast General Pharmaceutical Factory, Shenyang 110026, P. R. China*
[c]*Changchun Institute of Applied Chemistry, Chinese Academy of Sciences, Changchun 130022, P. R. China*

Received 9th August 2001, Accepted 24th January 2002
First published as an Advance Article on the web 20th February 2002

The first heteropoly acid–dipeptide complex, $(HGly\text{-}Gly)_3PMo_{12}O_{40}\cdot 4H_2O$, was synthesized and characterized by elemental analysis, IR, UV, ^1H NMR and single crystal X-ray diffraction. The X-ray crystallographic study showed that the crystal structure was constructed from N–H···O and O–H···O hydrogen bonds among the $(HGly\text{-}Gly)^+$, H_2O and $PMo_{12}O_{40}{}^{3-}$ units. This structure represents a model interaction between polyoxometalates and proteins. The complex has photosensitivity under irradiation by sunlight. The fluorescent activity of this compound is also reported.

1 Introduction

Applications of polyoxometalates as drugs against tumors and AIDS have increased the interest in the study of the association of polyoxometalates and proteins.[1] Various polyoxometalates are potent inhibitors of reverse transcriptase and other related enzymes.[2] To date, four of the HIV-1 protease inhibitors found in clinic use, Saquinavir, Inainavir, Ritonavir and Nelfinavir, are peptide-based compounds. They can inhibit either the protease or the complementary strand activity of the protease.[3]

Since the composition and structure of aqueous complexes are of direct relevance to the mechanism by which polyoxometalates interact with biological systems, characterization of such complexes is important for understanding the antitumor or anti-HIV activity. The interactions of amino acids or peptides with polyoxometalates have been noted previously.[4] Apart from the structural characterization of two isopoly acid salts, $(NH_4)_6(Gly\text{-}Gly)_2\cdot V_{10}O_{28}\cdot 4H_2O$ and $[Mo_4O_{12}(glycylglycylglycine)_2]\cdot 9H_2O$, no other structural information is presently available for peptides with heteropolyoxometalates at the molecular level. The present study provides new information on the structure of the compound $(HGly\text{-}Gly)_3PMo_{12}O_{40}\cdot 4H_2O$ (hereafter abbreviated as **1**), which is formed by the interaction between dodecamolybdophosphoric acid and the simple dipeptide glycylglycine (Gly-Gly).The structure of **1** represents a model interaction between polyoxometalates and proteins, which demonstrates that the most basic sites on the anion can be involved in hydrogen bonding.

2 Experimental

2.1 Synthesis

α-$H_3PMo_{12}O_{40}$[5] (3.0 g) was dissolved in 20 ml distilled water. With stirring, 20 ml HCl solution (0.5 mol dm^{-3} containing Gly-Gly 0.5 g) was added dropwise. The resulting yellow mixture was stirred for 10 h at room temperature, and the yellow solution formed was kept in a refrigerator (at 4 °C). Large quantities of light yellow block crystals were isolated after five days (yield 2.60 g, 69% based on $H_3PMo_{12}O_{40}$). Anal. calcd for $C_{12}H_{35}Mo_{12}N_6O_{53}P$: C, 6.28; H, 1.53; N, 3.66; P, 1.35; Mo, 50.22%. Found: C, 6.38; H, 1.46; N, 3.73; P, 1.31; Mo, 50.31%.

2.2 Physical measurements

C, H and N elemental analyses were performed on a Perkin-Elmer 240c elemental analyzer; P and Mo elemental analyses were performed on a PLASMA SPEC(I) quantometer. FT-IR spectra were recorded on a 5DX FT-IR spectrometer with KBr pellets. ^1H NMR spectra were obtained with a Bruker Am-500 spectrometer operating at 400 MHz using D_2O as solvent. The reflectance electronic absorption spectra were measured on a Cary 500 UV–Vis–NIR spectrophotometer. The EPR spectrum was recorded by means of a JES-Fe3AX spectrometer. The excitation and emission spectra were obtained on a SPEX FL-2T2 spectrofluorimeter with the slit at 0.8 mm and equipped with a 450 W lamp as the excitation source. X-Ray crystallographic data were collected on a Siemens P4 four-circle diffractometer in the ω-2θ scan mode. The surface of the crystal sample was coated with resin to avoid desolvation of the crystal. A semi-empirical absorption correction (PSISCAN) from ψ-scans was applied. The structure was solved by direct methods and refined by the full-matrix least-squares method on F^2 using SHELXTL-PLUS software. A summary of the crystallographic data and structural determination for **1** is provided in Table 1.

3 Results and discussion

3.1 Description of the structure†

The crystal structure determination of **1** showed that the compound consisted of $(HGly\text{-}Gly)^+$, H_2O, and $PMo_{12}O_{40}{}^{3-}$.

---

†CCDC reference number 168537. See http://www.rsc.org/suppdata/jm/b1/b107225k/ for crystallographic files in .cif or other electronic format.

DOI: 10.1039/b107225k

Table 1 Crystal data and structural refinement for **1**

Empirical formula	$C_{12}H_{35}Mo_{12}N_6O_{53}P$
Formula weight	2293.71
Temperature/K	293(2)
Wavelength/Å	0.71073
Crystal system	Triclinic
Space group	$P\bar{1}$
Unit cell dimensions	a = 12.455(3) Å, α = 100.13(3)° b = 13.057(3) Å, β = 102.79(3)° c = 16.840(3) Å, γ = 100.41(3)°
Volume/Å^3	2559.3(9)
Z	2
Density/mg m^{-3} (calculated)	2.976
Absorption coefficient/mm^{-1}	3.002
F(000)	2184
Crystal size/mm	0.52 × 0.38 × 0.32
θ range for data collection	1.63–25.01
Index ranges	$-1 \leq h \leq 14$ $-15 \leq k \leq 15$ $-20 \leq l \leq 19$
Reflections collected	10661
Independent reflections	8977 (R_{int} = 0.0300)
Refinement method	Full-matrix least-squares on F^2
Data/restrains/parameters	8977/0/760
Goodness-of-fit on F^2	1.079
Final R indices [$I > 2\sigma(I)$]	R_1 = 0.0347, wR_2 = 0.0955
R indices (all data)	R_1 = 0.0445, wR_2 = 0.0982
Large diff. peak and hole/e Å^{-3}	1.437 and −1.598

A fully labeled plot of the anion and the cations is given in Fig. 1a and 1b, respectively. The bond lengths and bond angles observed for the $PMo_{12}O_{40}{}^{3-}$ unit indicate that its geometry is quite similar to those found in previously reported dodecamolybdophosphoric acid salts.[6] It is a Keggin structure in which the central P atom is surrounded by a tetrahedron whose oxygen vertices are each linked to one of the four Mo_3O_{13} groups. Each Mo_3O_{13} consists of three MoO_6 octahedra linked in a triangular arrangement by sharing edges, and the four Mo_3O_{13} are linked together by sharing corners. The P–O bond lengths are in the normal range of 1.529(4)–1.540(4) Å. The Mo–O (terminal) and the Mo–O (bridge) bond lengths are in the range of 1.661(5)–1.686(5) and 1.842(4)–2.011(4) Å, respectively. The Mo–O–Mo bond angles vary between 88.5(2) and 155.5(2)°.

The structure of the [HGly-Gly]$^+$ cation is different from those of zwitterionic oligopeptides[7] and the Gly-Gly unit in $(NH_4)_6(Gly\text{-}Gly)_2{\cdot}V_{10}O_{28}$,[4b] which typically exhibit C–O (carboxylate) distances of ~1.25 Å. In **1** the C–O (carboxylate) distances are as follows: C11–O41 1.189(10), C11–O42 1.314(10), C21–O51 1.222(9), C21–O52 1.296(9), C31–O61 1.207(9) and C31–O62 1.319(9) Å. The magnitude and inequality (within experimental error) of these two C–O distances thus clearly indicate that the carboxylate group is protonated.

The bond angles in the Gly-Gly unit of **1** also compare favorably with corresponding parameters of free zwitterionic oligopeptides.[8] The angles C13–N11–C12 [122.5(6)°], C23–N21–C22 [121.1(6)°] and C33–N31–C32 [123.4(6)°] of the Gly-Gly unit in **1** are slightly (3.9–6.2°) larger than the usual ones, while N31–C32–C31 [111.2(6)°] is slightly (~4°) smaller than normal. The three dihedral angles between the plane of the peptide group (N21–C23–O53, N11–C13–O43 and N31–C33–O63) and the carboxylate group (O51–C21–O52, O41–C11–O42 and O61–C31–O62) are 60.9°, 62.6° and 48.3°, respectively, which are also unusual.[8] These changes may be caused by the interaction between the Gly-Gly unit and the polyanion.

Short N–H···O and O–H···O contacts were found between the oxygen atoms of the polyanion and the protons of Gly-Gly as is also seen in porphyrin and TTF-based cation radical salts.[9] Interatomic distances (Å) and angles involving hydrogen-bonded atoms are listed in Table 2. The observed C···O distances are in the range of 2.907–3.165 Å, which are comparable to those of the hydrogen-bonded cases cited above. Therefore, we think that hydrogen bonding is operative in the present crystals. Both types of oxygen atoms in the polyanions, *i.e.*, carbonyl and ether type, participate in hydrogen bonding.

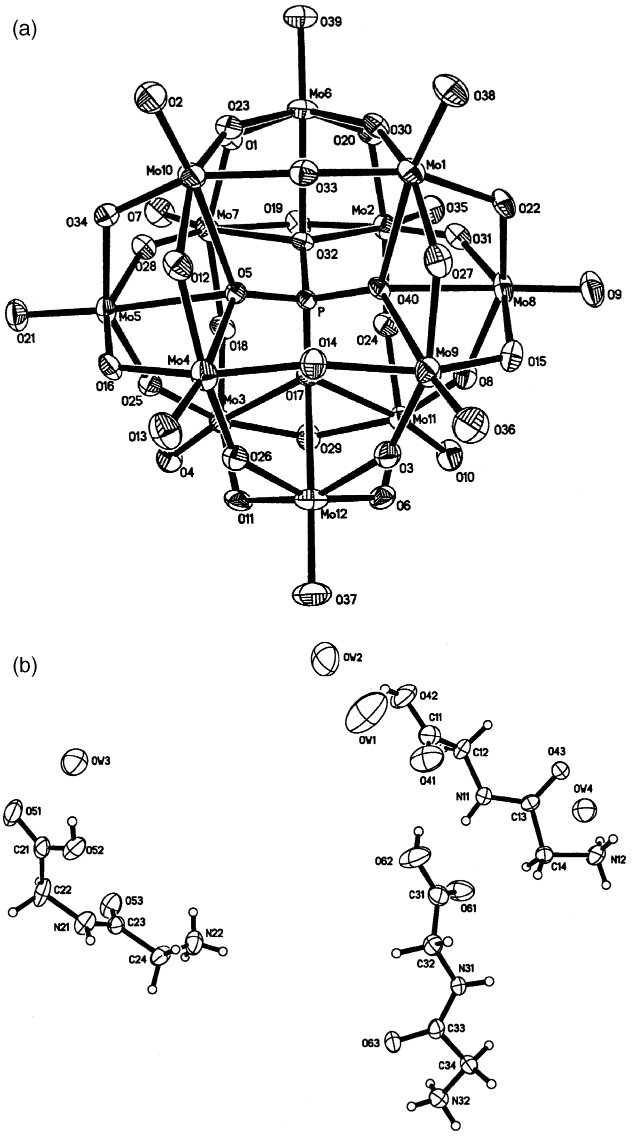

Fig. 1 (a) Structure and labeling scheme for $[PMo_{12}O_{40}]^{3-}$ (thermal ellipsoids at 50% probability). (b) View of the fully labeled cations [HGly-Gly]$^+$ in the structure of **1** (thermal ellipsoids at 50% probability).

It is interesting to observe that there are a number of short inter-species contacts in this structure. The representative ones are: O14···O38 (at $1 - x, -y, -z$) 2.771(7), O4···O6 (at $2 - x, -y, 1 - z$) 2.811 and O10···O35 (at $1 - x, -y, 1 - z$) 2.882(7) Å. The occurrence of these short contacts may be ascribed to hydrogen bonding between the polyanion and glycylglycine. As shown in Fig. 2, the structure of **1** seems to consist of a three-dimensional network *via* the short inter-species and hydrogen bonding. Along the [001] direction, the polyanions form a zigzag chain through O4···O6 and O10···O35 alternately [Fig. 2(b)].

3.2 FT-IR spectroscopy

The IR spectrum of the title compound is shown in Fig. 3. Characteristic peaks were observed for both the polyanion and the Gly-Gly countercation. The characteristic peaks at 793 (Mo–O$_c$–Mo), 879 (Mo–O$_b$–Mo), 960 (Mo–O$_d$) and 1061 cm^{-1} (P–O$_a$) demonstrate that $PMo_{12}O_{40}{}^{3-}$ is a Keggin structure. An

Table 2 Interatomic distances (Å) and angles (deg) involving hydrogen-bonded atoms in crystals of **1**

D–H···A	D–H	H···A	D···A	D–H···A	Symmetry operations for A
N11–H11···O34	0.86	2.49	2.979(6)	117	x, y, z
N11–H11···O61	0.86	2.30	3.031(5)	143	$1 + x, 1 + y, z$
N12–H12c···O9	0.89	2.54	2.907(7)	105	$2 - x, 1 - y, 1 - z$
N12–H12d···O24	0.89	2.47	3.087(8)	127	$2 - x, 1 - y, 1 - z$
N12–H12d···O29	0.89	2.40	3.099(8)	135	x, y, z
N12–H12c···OW4	0.89	2.08	2.929(6)	160	$x - 1, y, z$
N21–H21···O13	0.86	2.24	3.023(8)	152	x, y, z
N22–H22d···O22	0.89	2.16	2.987(7)	155	$1 - x, 1 - y, -z$
N22–H22e···O12	0.89	2.30	3.165(8)	165	$2 - x, 1 - y, 1 - z$
N31–H31···O4	0.86	2.06	2.899(8)	165	$2 - x, 1 - y, 1 - z$
N32–H32c···O39	0.89	2.63	3.164(7)	120	$1 - x, 1 - y, 1 - z$
N32–H32d···OW4	0.89	2.57	3.164(8)	114	$2 - x, 1 - y, 1 - z$
O42–H42···OW2	0.82	1.91	2.663(7)	153	x, y, z
O52–H52···OW3	0.82	1.90	2.714(7)	171	x, y, z
O62–H62···O41	0.82	2.01	2.799(8)	162	x, y, z
OW1···OW2			2.801(6)		

intense band at 1674 cm^{-1} could be ascribed to the C=O of the organic units. The intense peaks at 1634 and 1471 cm^{-1} are characteristic of $(NH_3)^+_{as}$ and $(NH_3)^+_s$ respectively.

3.3 ^{1}H NMR spectrum

The ^{1}H NMR spectrum of **1** is presented in Fig. 4. The ^{1}H chemical shifts of the two –CH_2– units in Gly-Gly are 3.854 and 4.036 ppm, respectively.

3.4 Solid state electronic spectrum

Fig. 5 compares the reflectance electronic spectra of $(HGly\text{-}Gly)_3PMo_{12}O_{40}\cdot 4H_2O$ (before irradiation) and $H_3PMo_{12}O_{40}\cdot nH_2O$. It was found that the low-energy absorption band undergoes a small shift, which is similar to the spectrum of $H_4SiW_{12}O_{40}\cdot 4HMPA$[10] and $H_3PMo_{12}O_{40}\cdot 6DMA\cdot CH_3CN\cdot 0.5H_2O$.[11] The results indicate that the interactions between Gly-Gly and $PMo_{12}O_{40}{}^{3-}$ are weak in the solid state.

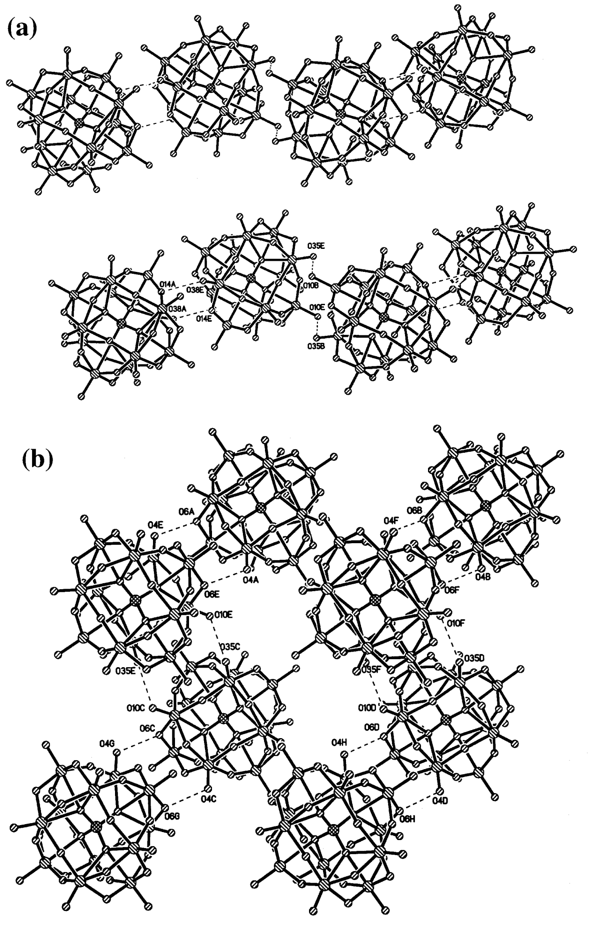

Fig. 2 View of the crystal packing of the title compound: (a) along the [100] direction; (b) along the [001] direction. All organic substrate and water molecules are omitted for clarity.

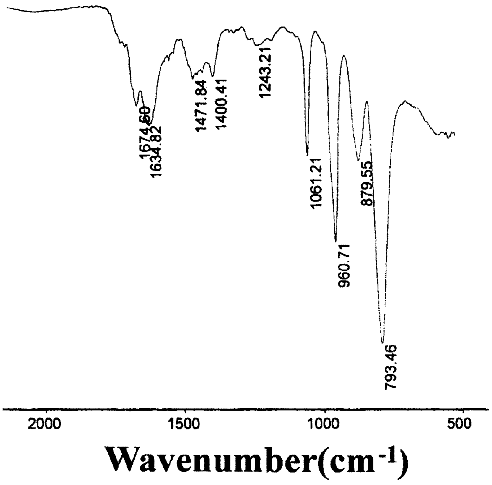

Fig. 3 IR spectrum of **1**.

3.5 Photochromism

Irradiation of pure title compound **1** by sunlight for 4 hours (28 °C, from 10:00 to 14:00) induces intense photochromism in the solid state. The solid reflectance electronic spectra of the irradiated and original samples are shown in Fig. 5. We found that the O → W charge transfer transition bands showed no evident changes in position, and only a small decrease in intensity. In addition, a new absorption band appeared in the

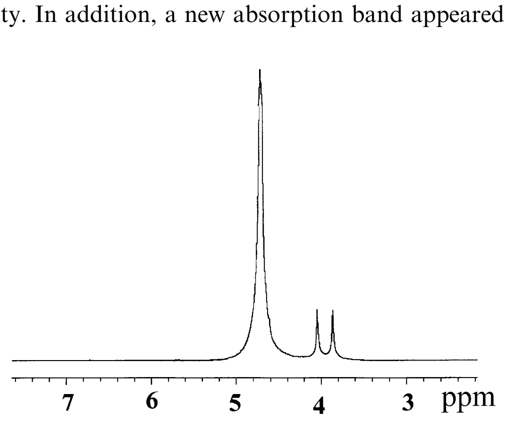

Fig. 4 ^{1}H NMR spectrum of **1**.

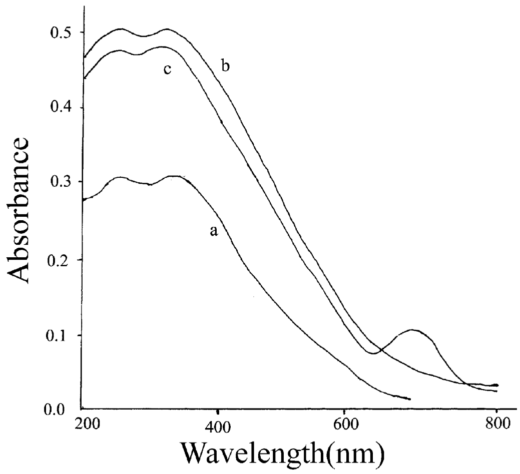

Fig. 5 Solid state electronic spectra of the compounds: (a) $H_3PMo_{12}O_{40}$; (b) $(HGly\text{-}Gly)_3PMo_{12}O_{40}\cdot 4H_2O$ and (c) $(HGly\text{-}Gly)_3PMo_{12}O_{40}\cdot 4H_2O$ after irradiation.

visible region, which is assigned to the intervalence charge transfer ($Mo^{5+} \rightarrow Mo^{6+}$) bands of the heteropoly anions and are characteristic bands of heteropoly blues.[12] This indicates that electron transfer occurs between the organic substrates and the heteropoly anions, which results in the reduction of the heteropoly anion ($Mo^{VI}O_6$) to heteropoly blue [$Mo^{V}O_5(OH)$]. This result has been verified by means of the EPR spectrum of the irradiated sample. No paramagnetic signals were observed in the EPR spectrum before irradiation, but some were observed at 77 K after irradiation. The paramagnetic signal of $(HGly\text{-}Gly)_3PMo_{12}O_{40}\cdot 4H_2O$ shown in Fig. 6 gives $g_\perp$ = 1.958 and $g_\parallel$ = 1.943, and this is the signal due to Mo^{5+}.

From the above results, it turns out that charge transfer between the organic substrates Gly-Gly and the molybdophosphoric anions can take place in compound **1** under the action of sunlight.

The photochromic mechanism can be described by the following equation,

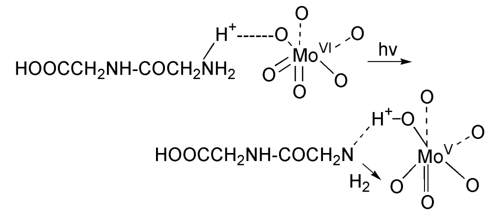

(1)

which is similar to the photochromic mechanism in alkylammonium polyoxomolybdate solids proposed by Yamase.[13] The photoexcitation of the O → Mo ligand-to-metal change-transfer (LMCT) band in the MoO_6 octahedra induces the transfer of a proton from a hydrogen-bonded amino nitrogen to a bridging oxygen atom at the photoreducible site in the edge-shared MoO_6 octahedral lattice. This is followed by the interaction of the d^1 electron with the proton that was transferred to the oxygen atom; simultaneously, the hole left at the oxygen atom as a result of the O → Mo LMCT transition interacts with the non-bonding electrons on the amino nitrogen atom to form a charge-transfer complex (**I**), in which a paramagnetic electron localized at the distorted $Mo^{V}O_5(OH)$ is responsible for the EPR signal. No radical signals were observed. Eqn. (1) depicts the environment of the photoreducible MoO_6 site and the subsequent formation of the charge-transfer complex (**I**) in the solid state; complex (**I**) reflects the separation of the electron and hole charges which are produced by the O → Mo LMCT transition in the polyoxomolybdate lattice. It is this charge separation that keeps the colored state stable. The blue solid can be changed to its original color in the dark by contact with ambient air or O_2, and cannot be decolored under an N_2 atmosphere. This shows that the decoloration process is an oxidation process, in which an electron is transferred from the Mo^V atom to the oxygen molecule, and not an oxidation–reduction process of complex (**I**) itself.

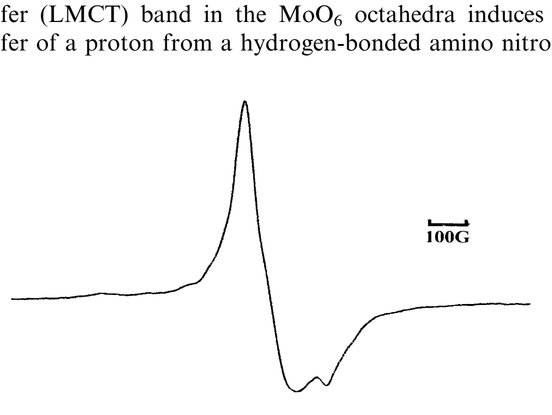

Fig. 6 EPR spectrum of the irradiated $(HGly\text{-}Gly)_3PMo_{12}O_{40}\cdot 4H_2O$ at 77 K.

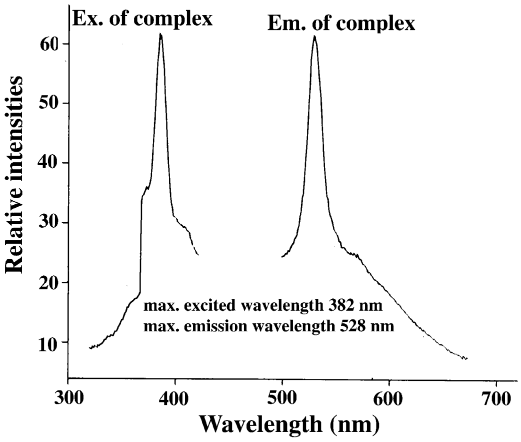

Fig. 7 Fluorescent emission spectrum of $(HGly\text{-}Gly)_3PMo_{12}O_{40}\cdot 4H_2O$ in the solid state.

3.6 Fluorescence spectrum

Photoexcitation of the oxygen-to-metal (O → M) ligand-to-metal charge-transfer (LMCT) bands of polyoxometalates generates an electron and a hole with d and 2p character, respectively. The return of the excited polyoxometalate to the ground state competes with the redox reactions of the excited state with electron acceptors or donors.[13] When several energies exist in the O → M LMCT bands, energy transfer occurs from the O → M LMCT excited state to these levels, as demonstrated for polyoxometaloeuropates.[14] A strong yellow fluorescent emission (at *ca.* 528 nm with an excitation wavelength of 382 nm) was observed for **1** (Fig. 7). However, this should be compared with the free ligand $H_3PMo_{12}O_{40}$, which showed green emission at *ca.* 510 nm, but measurement of its excitation maximum was difficult owing to its weak emission.[15] The increased emission of **1** probably relates to the hydrogen bonding and to the interaction of the short O···O contacts of between species. Fluorescent emission of **1** makes it a potential candidate for bio-sensing applications on the basis of recognition of appropriate guest molecules.

Acknowledgement

We thank the National Natural Science Foundation of China for financial support (20171010).

References

1 (*a*) J. T. Rhuie, C. L. Hill and D. A. Judd, *Chem. Rev.*, 1998, **98**, 327 and references cited therein; (*b*) E. B. Wang, C. W. Hu and L. Xu, *Concise Polyoxometalates*, Chemical Industry, Beijing, 1997, p. 146; (*c*) Y. Inouye, Y. Tokutake, T. Yoshida, Y. Seto, H. Huijita, K. Dan, A. Yamamoto, S. Nishiya, T. Yamase and S. Nakamura, *Antiviral Res.*, 1993, **20**, 317; (*d*) D. C. Crans, *Comments Inorg. Chem.*, 1994, **16**, 35.

2 C. L. Hill, M. S. Weeks and R. F. Schinazi, *J. Med. Chem.*, 1990, **33**, 2767.

3 X. Q. Zhang and J. Fan, *HIV Infection and AIDS*, People Heath Press, Beijing, 2000, p. 230.

4 (*a*) D. C. Crans, *Comments Inorg. Chem.*, 1994, **16**, 1; (*b*) D. C. Crans, M. Mahroof-Tahir, O. P. Anderson and M. M. Miller, *Inorg. Chem.*, 1994, **33**, 5586; (*c*) T. Yamase, M. Inoue, H. Naruke and K. Fukaya, *Chem. Lett.*, 1999, **6**, 563; (*d*) M. Inoue and T. Yamase, *Bull. Chem. Soc. Jpn.*, 1996, **69**, 2863; (*e*) J. H. Liu, J. Peng and E. B. Wang, *J. Mol. Struct.*, 2000, **525**, 71.

5 H. Wu, *J. Bio. Chem.*, 1920, **43**, 189.

6 (*a*) J. F. Keggin, *Proc. R. Soc. London, Ser. A*, 1934, **144**, 75; (*b*) J. F. Keggin, *Nature*, 1933, **131**, 908; (*c*) L. H. Bi, E. B. Wang, L. Xu and R. D Huang, *Inorg. Chim. Acta*, 2000, **305**, 163.

7 C. Djordjevic, M. Lee and E. Sinn, *Inorg. Chem.*, 1989, **28**, 719.

8 R. E. Marsh and J. Donohue, in *Advances in Protein Chemistry*, Academic Press, New York, 1967, p. 235.

9 (*a*) K. Sugiura, Y. Sakata, T. Tanaka and M. Sawada, *Chem. Lett.*, 1997, **3**, 281; (*b*) C. J. Gomez-Garcia, C. Gimenz-Saiz, S. Triki, E. Coronado, P. L. Magueres, L. Ouahab, L. Ducasse, C. Sourisseau and P. Delhase, *Inorg. Chem.*, 1995, **34**, 4139.

10 J. Y. Niu, X. Z. Xiao and C. Y. Duan, *Inorg. Chem.*, 1996, **35**, 4211.

11 M. M. Williamson, D. A. Bouchard and C. L. Hill, *Inorg. Chem.*, 1987, **26**, 1436.

12 (*a*) M. T. Pope, *Heteropoly and Isopoly Oxometalates*, Springer, Berlin, 1983, p. 321; (*b*) E. B. Wang, L. Xu and C. W. Hu, *Chin. Sci. Bull.*, 1991, **20**, 1544.

13 T. Yamase, *Chem. Rev.*, 1998, **98**, 307.

14 (*a*) T. Yamase, H. Naruke and Y. Sasaki, *J. Chem. Soc., Dalton Trans.*, 1990, 1687; (*b*) T. Yamase and H. Naruke, *J. Chem. Soc., Dalton Trans.*, 1991, 285; (*c*) M. Sugeta and T. Yamase, *J. Lumin.*, 1991, **50**, 50; (*d*) H. Naruke and T. Yamase, *Coord. Chem. Rev.*, 1991, **111**, 83.

15 T. Yamase and M. Sugeta, *J. Chem. Soc., Dalton Trans.*, 1993, 759.